SANDIA REPORT
SAND2007-0417
Unlimited Release
Printed February 2007

Advancement in Thermal Interface Materials for Future High-Performance Electronic Applications: Part 1

Michael J. Rightley, John A. Emerson, C. Channy Wong, Dale L. Huber,
and Blake Jakaboski

Prepared by
Sandia National Laboratories
Albuquerque, New Mexico 87185 and Livermore, California 94550

Sandia is a multiprogram laboratory operated by Sandia Corporation,
a Lockheed Martin Company, for the United States Department of Energy's
National Nuclear Security Administration under Contract DE-AC04-94AL85000.

Approved for public release; further dissemination unlimited.

Issued by Sandia National Laboratories, operated for the United States Department of Energy by Sandia Corporation.

NOTICE: This report was prepared as an account of work sponsored by an agency of the United States Government. Neither the United States Government, nor any agency thereof, nor any of their employees, nor any of their contractors, subcontractors, or their employees, make any warranty, express or implied, or assume any legal liability or responsibility for the accuracy, completeness, or usefulness of any information, apparatus, product, or process disclosed, or represent that its use would not infringe privately owned rights. Reference herein to any specific commercial product, process, or service by trade name, trademark, manufacturer, or otherwise, does not necessarily constitute or imply its endorsement, recommendation, or favoring by the United States Government, any agency thereof, or any of their contractors or subcontractors. The views and opinions expressed herein do not necessarily state or reflect those of the United States Government, any agency thereof, or any of their contractors.

Printed in the United States of America. This report has been reproduced directly from the best available copy.

Available to DOE and DOE contractors from
U.S. Department of Energy
Office of Scientific and Technical Information
P.O. Box 62
Oak Ridge, TN 37831

Telephone: (865) 576-8401
Facsimile: (865) 576-5728
E-Mail: reports@adonis.osti.gov
Online ordering: http://www.osti.gov/bridge

Available to the public from
U.S. Department of Commerce
National Technical Information Service
5285 Port Royal Rd.
Springfield, VA 22161

Telephone: (800) 553-6847
Facsimile: (703) 605-6900
E-Mail: orders@ntis.fedworld.gov
Online order: http://www.ntis.gov/help/ordermethods.asp?loc=7-4-0#online

SAND2007-0417
Unlimited Release
Printed February 2007

Advancement in Thermal Interface Materials for Future High-Performance Electronic Applications: Part 1

Michael J. Rightley, John A. Emerson, C. Channy Wong, Dale L. Huber, and Blake Jakaboski

Advanced Microsystem Packaging Department, Organic Materials Department, Microscale Science & Technology Department, CINT Science Department

Sandia National Laboratories
PO Box 5800
Albuquerque, NM 87185-1245

Abstract

As electronic assemblies become more compact and increase in processing bandwidth, escalating thermal energy has become more difficult to manage. The major limitation has been nonmetallic joining using poor thermal interface materials (TIM). The interfacial, versus bulk, thermal conductivity of an adhesive is the major loss mechanism and normally accounts for an order magnitude loss in conductivity per equivalent thickness. The next generation TIM requires a sophisticated understanding of material and surface sciences, heat transport at submicron scales, and the manufacturing processes used in packaging of microelectronics and other target applications. Only when this relationship between bond line manufacturing processes, structure, and contact resistance is well-understood on a fundamental level will it be possible to advance the development of miniaturized microsystems. This report examines using thermal and squeeze-flow modeling as approaches to formulate TIMs incorporating nanoscience concepts. Understanding the thermal behavior of bond lines allows focus on the interfacial contact region. In addition, careful study of the thermal transport across these interfaces provides greatly augmented heat transfer paths and allows the formulation of very high resistance interfaces for total thermal isolation of circuits. For example, this will allow the integration of systems that exhibit multiple operational temperatures, such as cryogenically cooled detectors.

ACKNOWLEDGMENTS

The authors gratefully acknowledge the supported by Laboratory Directed Research and Development program at Sandia National Laboratories. Jeffrey Galloway made early significant contributions to the idea of measuring an effective thermal interface. We are most grateful for the contributions of Ed Piekos and Frank van Swol.

CONTENTS

FIGURES

TABLES

NOMENCLATURE

bcc	body-centered cubic
EMA	effective medium approximation
fcc	face-centered cubic
FEA	finite element analysis
LDRD	Laboratory Directed Research and Development
SNL	Sandia National Laboratories
TIM	thermal interface materials

1. OVERVIEW

1.1 The Problem

The trend in microsystems is to reduce volume and power levels by increasing the level of integration and through standard size reductions in ASIC and other electronic components. This process has seen greater relative gains in the size/volume reductions than in the power reductions of electronic components. The result has been a steadily increasing thermal management challenge coincident with a significant reduction in the spatial dimensions that are typically used to spread and dissipate heat. Additionally, as characteristic dimensions are continuously reduced, the heat transfer pathways are so impacted that even the dominant heat transfer modalities are varied (i.e., conduction is severely limited in very thin devices, radiation becomes more important as the view factors are increased, and convection becomes negligible as it is based on heated surface area).

One unforeseen consequence of this trend has been a drastic increase in the importance of the interface to the overall thermal problem. Spreading resistance can be minimized by thinning of the heat producing device, but the unfortunate reality is that this drives the relative contribution of the interfacial resistance upwards. This trend has already reached a point where use of very high thermal conductivity materials for device substrates and heat sinks doesn't help to lower the junction temperature of the device due to the significant thermal resistance of the interface; both the contact resistances and the conductivity of the die attach material itself. These polymer-based epoxies typically demonstrate thermal conductivity on the order of 0.1 W/mK.

Material formulators, sensing this trend early, have already started infusing their products with metal materials (flakes, spheres, etc.) at the microscale to boost their thermal conductivities. Now referred to as thermal interface materials (TIMs), these "metal-loaded" epoxies pay a penalty in viscosity and adhesive quality to incorporate the higher conductivity materials. Studies to maximize the conductivity of these epoxies have shown inverse relationships between the adhesive and thermal performances. Currently, it appears that the volume fractions of microscale metal particles in these epoxies are, at a maximum, based on the amount of adhesive and flow degradation observed.

Efforts to create high-conductivity, all-metallic adhesives, so-called solder or eutectic bonds, have been progressing with some success. These bonds require fundamentally different application processes and can strain thermal budgets for the attached devices. As a result, there is still a vigorous effort to improve the filled polymer systems (Mahajan 2002).

1.2 Heat Transfer in a Polymer Epoxy

Wetting and squeeze flow studies have demonstrated that metal-loaded polymer epoxies experience aggregation of the metal particles into the center of the material and away from the two interfaces as a result of fluidic forces and interactions during the flow. Figure 1 illustrates the concept using spheres for the shape of the metal particles.

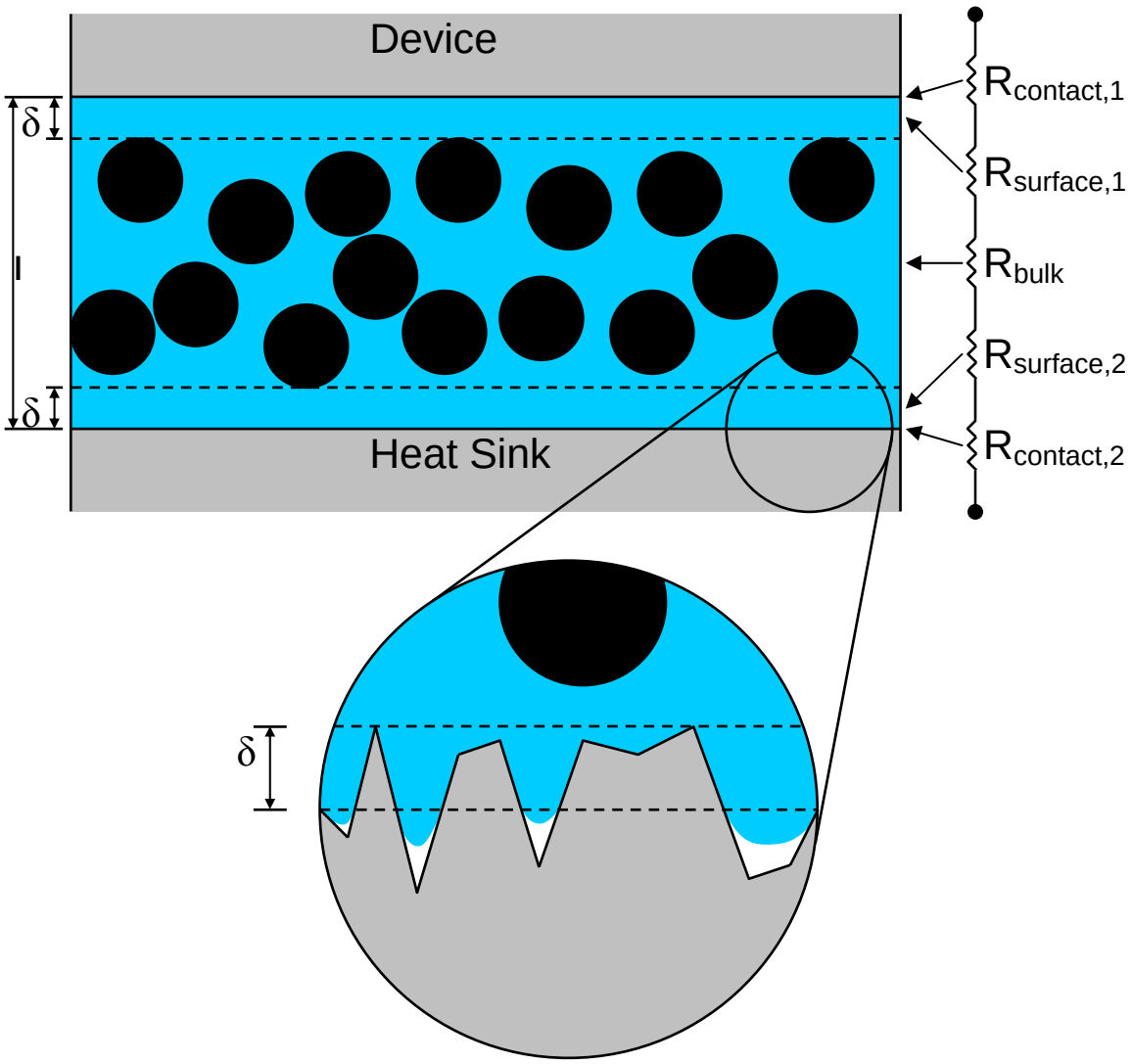

Figure 1. Cured state of metal loaded epoxy.

It has been observed that the predicted thermal conductivity of such a bimorph epoxy, using standard acoustic theory, is roughly one order of magnitude larger than the measured values. Figure 1 makes clear the nature of this discrepancy. To obtain the full benefit of the metal particles, it is necessary for many of them to have robust thermal contact with each other and with the two opposing surfaces across which heat is intended to flow. Squeeze flow results indicate that contact of metal particles to either surface will not happen in a manner that allows this heat transfer. As a result, the effective thermal conductivity is still very close to that of the polymer material itself.

Some have postulated that an additional material (Prasher 2005) of high thermal conductivity but at a significantly smaller spatial dimension could bridge the thermal gap across to the two surfaces without significantly degrading the flow and adhesion performance of the polymer. This increased thermal connectivity would allow the material to exhibit bulk conductivity values that could be significantly higher than the standard microscale metal loaded material.

The augmentation of a microscale, metal-loaded epoxy with nanoscale metallic particles is the subject of this report. Figure 2 illustrates the concept.

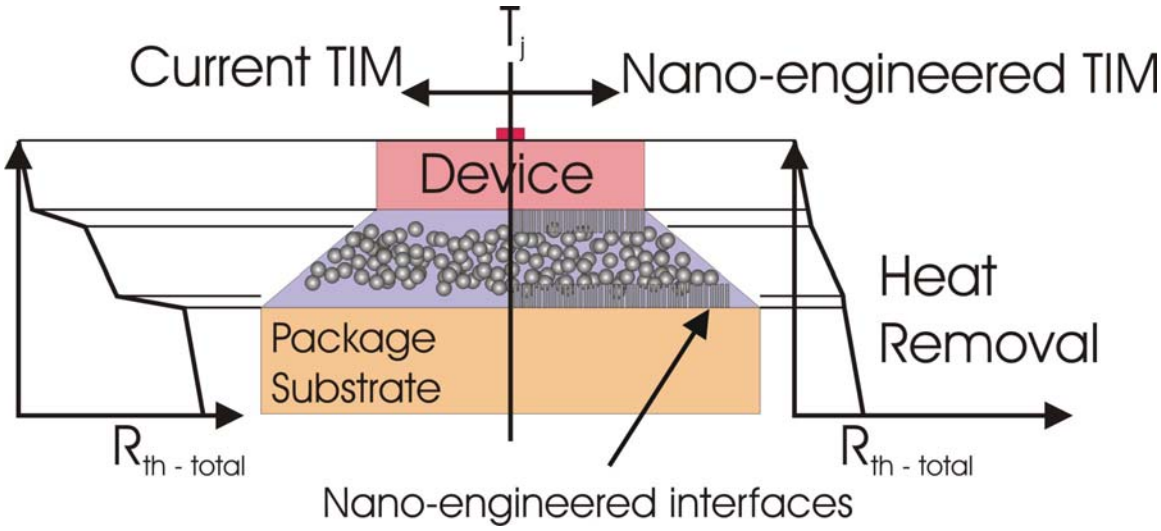

Figure 2. Nanoparticle-augmented TIM.

2. MODELING AND PHYSICS

2.1 Introduction/Motivation

Different types of fillers with high electrical and thermal conductivities, e.g. graphite and alumina, have been added to adhesive polymers to create composite materials with improved mechanical and electrical properties. Previous modeling efforts have found that it is relatively difficult to predict the effective thermal conductivity of a composite polymeric material when incorporated with large volume content of filler. For small volume content of filler, the effective thermal conductivity of the composite material generally increases linearly with an increasing volumetric fraction. The Maxwell-Eucken model can predict the effective thermal conductivity of this composite material. However, for large volume content of filler, the thermal conductivity behaves nonlinearly with the volumetric fraction. Further experimental investigations have determined that at small volume content, the filler is likely evenly dispersed in the homogeneous phase of the matrix. Hence, they are hardly touching each other. This structure is known as the 'dispersed' phase. Many analytical and numerical models have been developed for this dispersed phase and are available in the open literature. At high volume content, it is likely that some filler is touching others and forming conductive chains of filler. These conductive chains, if aligned along the direction of the temperature gradient, will create a preferable path for heat transfer. This arrangement of filler, in the 'attached' phase, subsequently leads to a drastic increase in the effective thermal conductivity of the composite material.

2.1.1 Agari Experiment

Many experiments have been conducted to determine the impact of incorporating filler to enhance the heat transfer process. This section focuses on the results of two Agari experiments used to assess the computational models being developed.

- The measured thermal conductivity of three composites: polyethylene with carbon black, polyethylene with graphite filler, and polyvinyl chloride with graphite filler have been reported in the literature (Agari 1985). Maximum volume content of graphite was about 30%. Data started to deviate from Maxwell-Eucken equation at about 10% volumetric fraction. At large volume content of filler, the measured value was much higher than the prediction using existing correlations.
- Agari (Agari 1990) measured the thermal conductivity of polyethylene and polystyrene composites filled with high volume content of quartz or alumina particles. At above 30% volume content, these fillers start to interact with each other and form an 'attached' system. Semiempirical correlation has been developed to fit the data obtained from experiments.

Both the 1985 and 1990 sets of data will be used to validate the computational results presented in this section.

2.1.2 Existing Models

Many analytical and numerical models work well for the disperse phase; these model predictions are reliable as long as the filler is homogeneously dispersed. However, if the filler is in the attached phase, only a few models show promising results.

- Maxwell and Rayleigh developed the "effective medium approximation (EMA)" model. This model assumes an isotropic distribution of fillers. Since then, many modifications have been added to this model, making it increasingly sophisticated. Recent versions include shape, size effects, and interfacial resistance. However, these models are unable to predict the effective thermal conductivity accurately if touching between filler particles exists.
- Agari (1986) used a generalization of parallel and series conduction models to estimate the thermal conductivities of filled polymers. His modified model considered the fillers being randomly dispersed and predicted an isotropic thermal conductivity with moderate success at low volume content.
- Agari (1990) provided an assessment of many model predictions and their comparison with experimental data at high volume fraction. Discrepancy existed, especially at high volume content of filler. General observation was that empirical correlations did not capture well the structural complexity of the composite materials.
- Hatta and Taya (1986) solved the heat conduction equation of a coated-fiber embedded in an infinite matrix subjected to a far-field heat flux using an analytical model. Analytical solutions for both single and multiple fibers were developed. No clear closed-form solution could be generated for high volume fraction with touching fibers.
- Davis and Artz (1995) used finite element analysis (FEA) to investigate heat conduction of composite with bimodal distributions of particle size. Prediction is reliable as long as filler particles are not touching others.
- Contact resistance between matrix and particles (Kapitza resistance) was investigated by Hasselman and Johnson (1987). They developed formulas for spherical, cylindrical, and flat-plate geometry to predict an effective thermal conductivity of composites with interfacial thermal barrier resistance. The model worked well for a much diluted system. If the interfacial resistance was zero or infinite, particle size effect on the effective thermal conductivity was minimal. For a finite resistance, decreasing the particle size usually decreased the effective thermal conductivity for a given volume content. Hence, just incorporating nanoparticles of the same size in a composite system might not work, but adding nanoparticles only in the depletion zone of a composite with filler of microns in diameter should be analyzed.

2.2 Computational Analysis Tools

A set of computational tools developed at Sandia National Laboratories (SNL) has been applied to model the heat conduction across the TIMs and calculate the effective thermal conductivity of the composite for different volume contents of filler. The analysis procedure involves: (1) generating a computational geometric model representing the structure of the composite; (2) simulating the heat transfer across the composite for a set of boundary conditions using a finite element thermal analysis tool; and (3) calculating and evaluating the results.

2.2.1 Cubit – A Computational Mesh Generator

CUBIT is a 2-D or 3-D finite element mesh generation toolkit for solid models (Shepherd, 2000). Usually a geometry file can be ported into CUBIT to generate a computation mesh system for analysis. It can produce quadrilateral and hexahedral meshes, as well as triangle, tetrahedral, and hex-dominant meshes. CUBIT follows a toolkit approach, offering a variety of meshing techniques: 2-D and 3-D mapping, multiple sweeping, paving, and the latest meshing techniques, such as plastering, whisker weaving and grafting. It runs on both UNIX and PC platforms.

In addition to mesh generation, CUBIT has some basic features to construct a 3-D solid model that meets the needs of the SNL team. Other complex solid modeling capabilities include advanced geometry creation and modification, Boolean operations, web-cutting, healing, auto decomposition, defeaturing, and nonmanifold topology.

2.2.2 Calore – A Finite Element Thermal Analysis Program

Calore is a computational program for transient 3-D heat transfer analysis (Bova 2005). It is built upon the SIERRA finite element framework to run on both desktop and parallel computers (Edwards and Stewart, 2001). Advanced thermal analysis capabilities include anisotropic conduction, enclosure radiation, thermal contact, and chemical reaction. The governing energy conservation equation in Calore is expressed as follows:

$$\frac{\partial}{\partial t}(\rho \cdot c \cdot T) + \sum_{i=x,y,z} \frac{\partial}{\partial x_i}(\rho \cdot c \cdot u_i \cdot T) = \sum_{i=x,y,z} \frac{\partial}{\partial x_i}(q_i) + S \qquad (1)$$

where $q_i = -\sum_{j=x,y,z} k_{ij} \frac{\partial T}{\partial x_j}$;

ρ = density;
c = heat capacity;
T = temperature;
u_i = convective velocity;
q = heat flux;
S = volumetric heat generation rate.

Boundary conditions available include specified temperature, heat flux, force or free convection, and surface radiation.

Calore also has many state-of-the-art computational features, such as element death, automatic selection of the time step size, mesh adaptivity, and dynamic load balancing for massively parallel computing.

2.3 Code Validation and Modeling Strategy

According to the experimental findings, for a given volume content of filler, the measured thermal conductivity of the composite is reasonably repeatable, even though the filler is randomly distributed in the adhesive polymers. These measured values statistically follow a normal distribution with a very small standard deviation, provided that the samples are produced

from a well-controlled and consistent manufacturing process. This section assesses the computational model by comparing its predictions against measurement.

The computational model in the initial analysis has the filler randomly distributed. For a low volume content of filler, the numerical algorithm that searches and places filler particle into an open space within a defined volume works very well. However, when the volume content of filler gets too large, the 'search-and-place' algorithm becomes inefficient and time-consuming. To overcome this deficiency, a new numerical algorithm was developed that has filler initially distributed in a crystallographic structure, such as face-centered cubic (fcc) or body-centered cubic (bcc) crystal structure. Then for the next hundred iterations, it allows the filler to move randomly. This approach works well to build a computational model and calculate an effective thermal conductivity of a composite. Nevertheless, randomly distributed filler particles have a drawback. It generates significant variations in the calculated thermal conductivity due to the randomness of filler distribution (first three Columns in Table 1). A large number of simulations is needed to suppress the noises and calculate an average value. Obtaining an average is important to recognize the pattern of thermal conductivity behavior as a function of volume content of filler.

Table 1. Calculated Effective Thermal Conductivity of Composite Materials with Filler Particles Distributed in Different Configurations.

Distribution	Random 1	Random 2	Random 3	BCC	FCC
Void Fraction	34.68%	35.48%	34.47%	32.66%	33.53%
Thermal Conductivity	0.007077 W/cm K	0.007480 W/cm K	0.007150 W/cm K	0.006975 W/cm K	0.007185 W/cm K

Since the goal is to understand how incorporating filler will enhance the heat conduction across the composite material, a more deterministic approach is required. Hence, a structured filler distribution becomes attractive for the analysis. A structured distribution implies that the filler is arranged in a crystallographic orientation, such as fcc or bcc structure (Figure 3), instead of an unstructured distribution with filler being randomly scattered (Figure 4). Table 1 shows the calculated effective thermal conductivities of composite materials with different filler distributions, but similar volume content of filler. The calculated values for different filler distributions are reasonably close to each other, implying that the filler distribution effect may be secondary to the primary goal of this investigation. These results are for the composite material with filler scattered, yet not touching.

Unless it is mentioned, the following results are for the composite materials with filler distributed in a crystal lattice orientation. The goal is still to better understand how size, volume content, and distribution will affect the effective thermal conductivity of a composite material. It is assumed that for a given volume content of filler, the thermal conductivity of a composite with filler distributed in a crystal lattice structure is qualitatively similar to those with filler distributed randomly, as shown in Table 1. The first set of analyses is for the polyethylene composite filled with graphite filler. This composition is investigated by Agari (1985). The calculated thermal conductivity of this composite as a function of volume content of graphite filler is compared

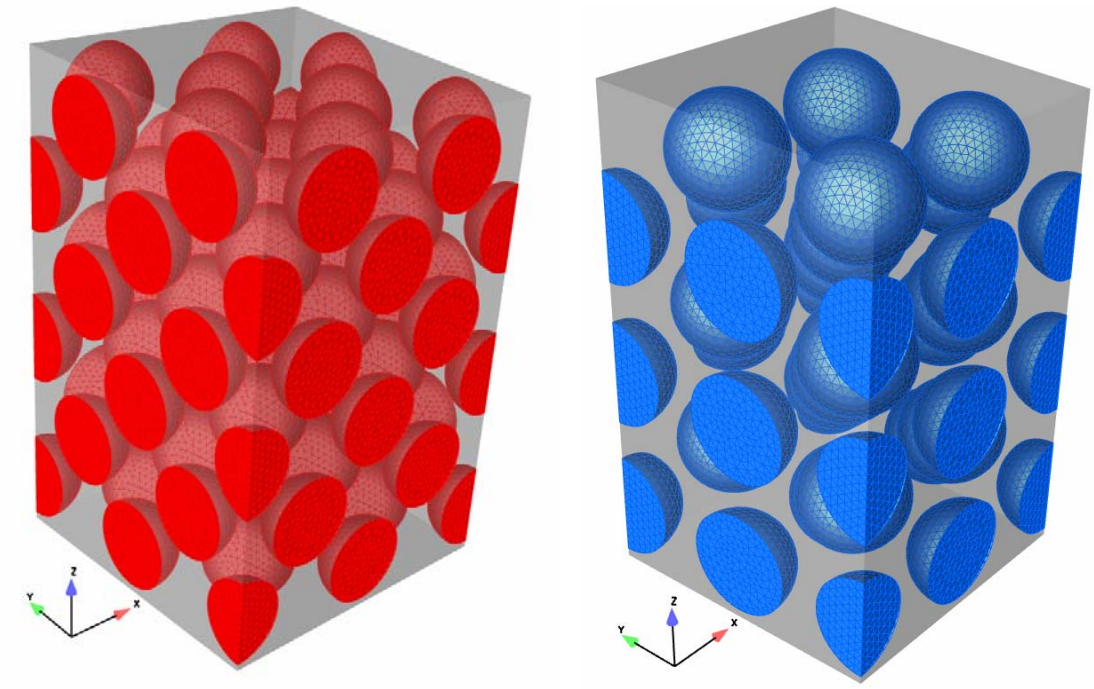

Figure 3. (Left) Filler in the face-centered cubic lattice structure and (Right) filler in the body-centered cubic lattice structure.

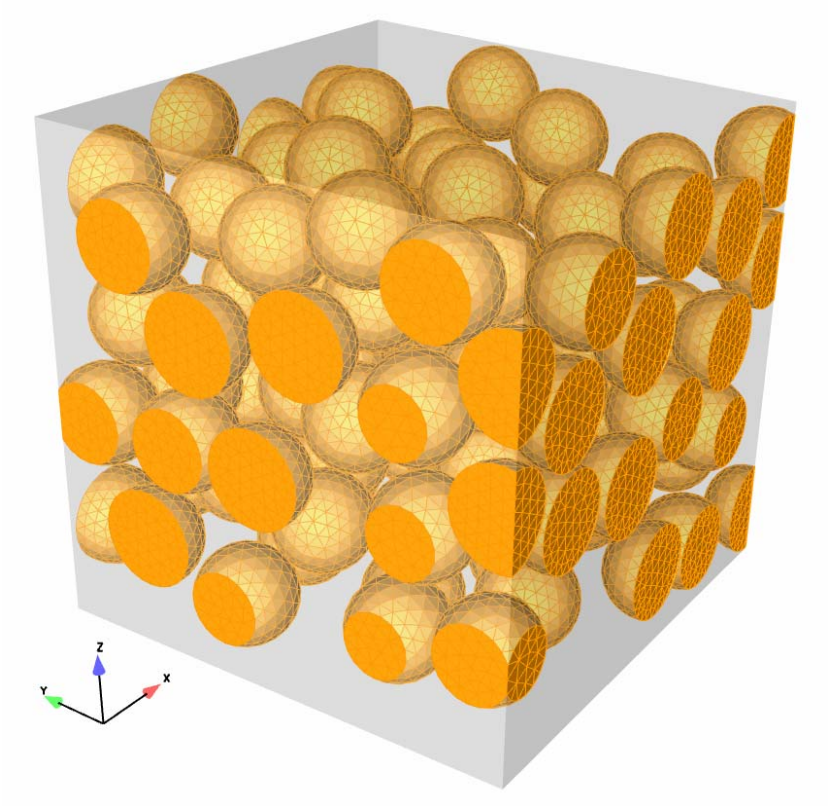

Figure 4. Filler distributed randomly.

against the experimental data (Figure 5). Prediction using the Maxwell-Eucken equation is also included in this plot for comparison. The computational model has the filler set up in a bcc lattice structure. Results from both FEA and correlation match well with each other. However, they both compare reasonably well against measurement at the low volume content, but fail at the moderate volume content. One explanation of this discrepancy is that at moderate volume content, the filler will be in the attached phase in experiment, while the filler in the models is in the dispersed phase.

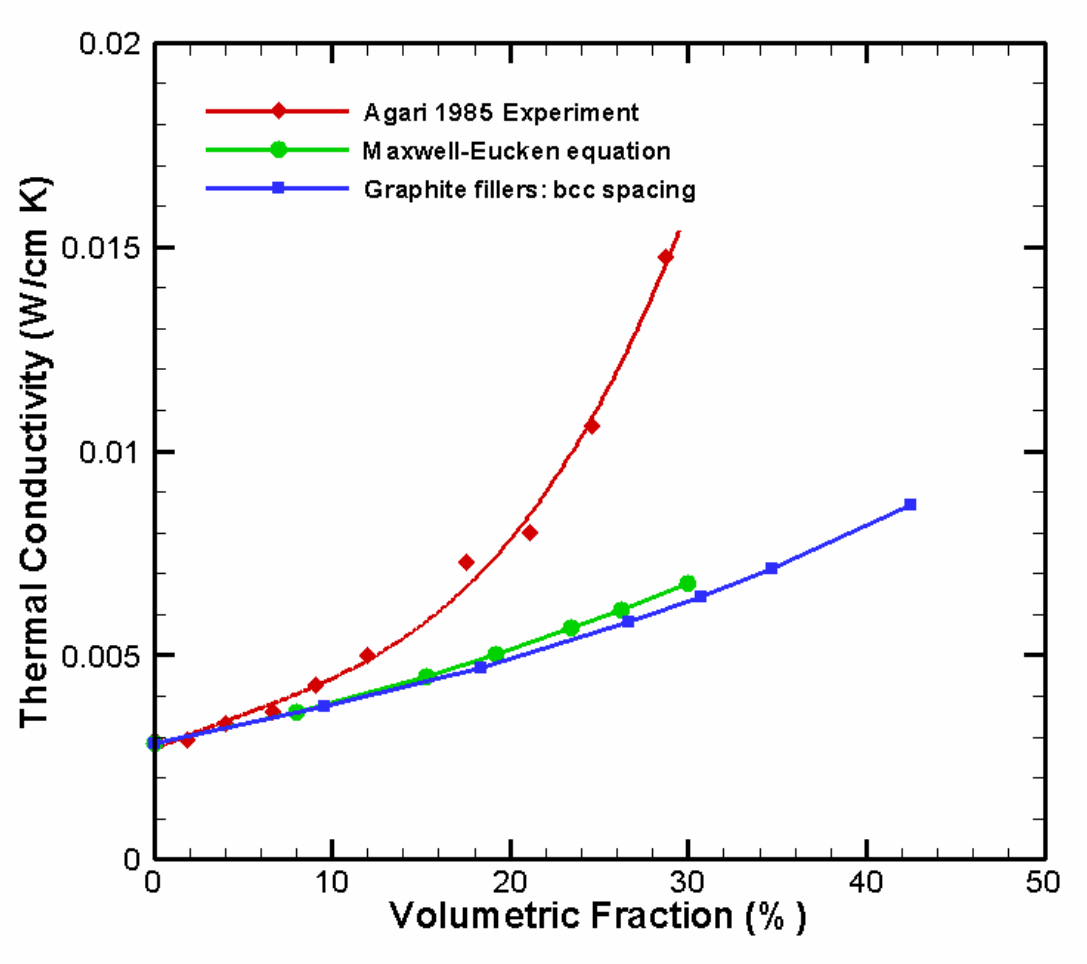

Figure 5. Comparing predictions against measurement for a polyethylene composite with graphite filler.

The next set of comparison is for the polyethylene composite with alumina filler. Results from simulations in which the filler is set up in both fcc and bcc lattice structure are compared against data from the Agari (1990) experiment. At low and moderate volume content of filler, predictions compare reasonably well with measurement. At the volumetric fraction of 45% or above, there is a drastic increase in the effective thermal conductivity, implying that a large percentage of filler will be in the attached phase. In the computational model, except at the volumetric fraction of 60% or above, the filler is in the dispersed phase. That is, each filler particle does not touch others.

2.4 Modeling Filler in the Attached Phase

When a group of filler particles are in contact with one another, forming a chain of attached filler particles in the direction of temperature gradient (Figure 7), the effective thermal conductivity can drastically increase. This effect is predicted especially for those cases when the volume content of filler is very high. For the composite with filler in the bcc lattice structure, the drastic increase of conductivity occurs at the volumetric fraction of about 60% (at the last data point in Figure 6). Similarly, for the composite with filler in the fcc lattice structure, the drastic increase occurs at the volumetric fraction of about 65% (Figure 6).

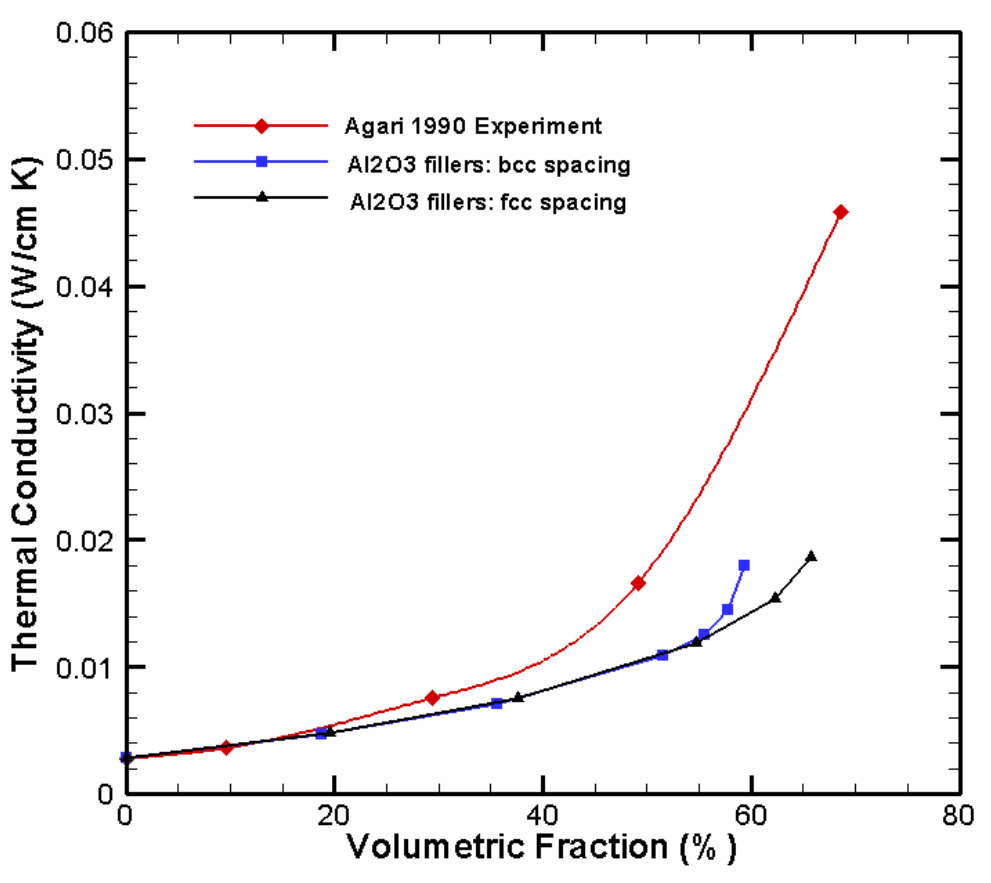

Figure 6. Comparing predictions against measurement for a polyethylene composite with alumina filler.

When chains of attached filler are created in the direction of temperature gradient, a preferable path for heat conduction will be generated, leading to a significant reduction of temperature at the hot spot. Hence, the effective thermal conductivity of the composite is much higher. This physical phenomenon can be shown in the following demonstration. In these two thermal analyses, the computational model is set up so that six rows of filler particles are arranged in a bcc lattice formation. One is in the dispersed phase and the other is in the attached phase. The volume content of filler is about 55%. In order to create chains of attached filler at this moderate volume content, a portion of the filler particles are shifted from the original position to the new

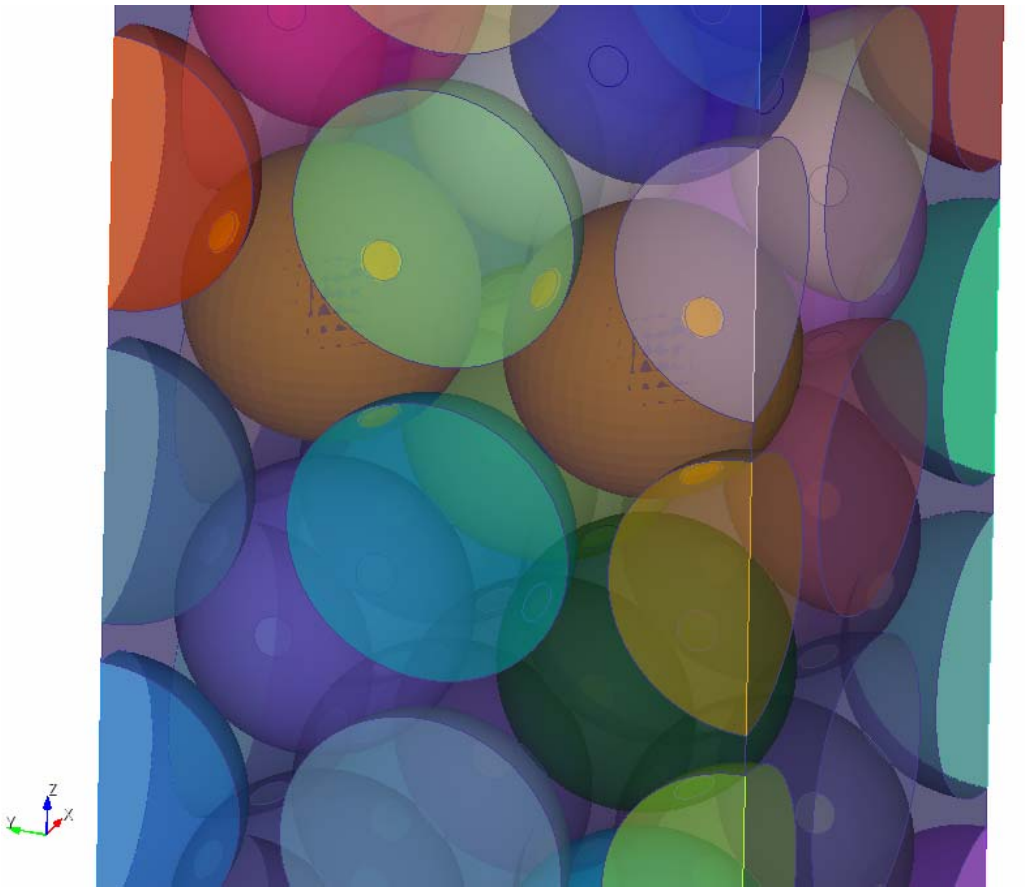

Figure 7. Picture of the filler in the attached phase. Two interior filler particles are highlighted to illustrate the small circles which are the common contact areas between neighboring filler particles.

position, creating contacts between particles. In this attached system, multiple chains of six filler particles attached somewhat vertically have been created.

Figure 8 plots the temperature contour of the composite with filler. A surface heat flux is applied at the top surface and a constant temperature is maintained at the bottom surface. More information on the problem setup can be found in Appendix A. Also included in the plot is the axial temperature distribution across the thickness of the composite. The axial temperature plot illustrates that a significant temperature gradient exists across the adhesive polymer between filler particles, even though it is very thin. Since polymer is a relatively poor thermal conductive material, it retards the heat transfer process. When the filler is in the attached phase, the temperature gradient is relatively small in majority of the region. A large temperature gradient only occurs at the depletion zones located near the top and bottom surfaces (Figure 9).

The temperature at the top surface is not uniform, so there is a need to determine what temperature is used to calculate the effective thermal conductivity. In the present analysis, the maximum temperature instead of the average temperature is applied. This approach will lead to a smaller value of thermal conductivity.

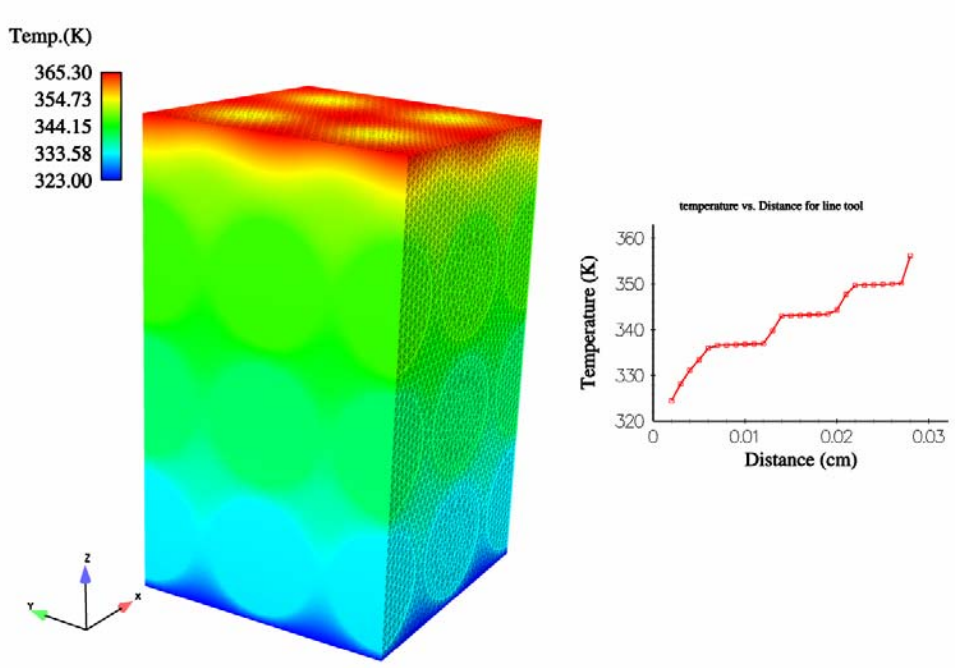

Figure 8. **(Left) Temperature contour plot of the composite with filler distributed in the disperse phase; (Right) Axial temperature distribution across the composite.**

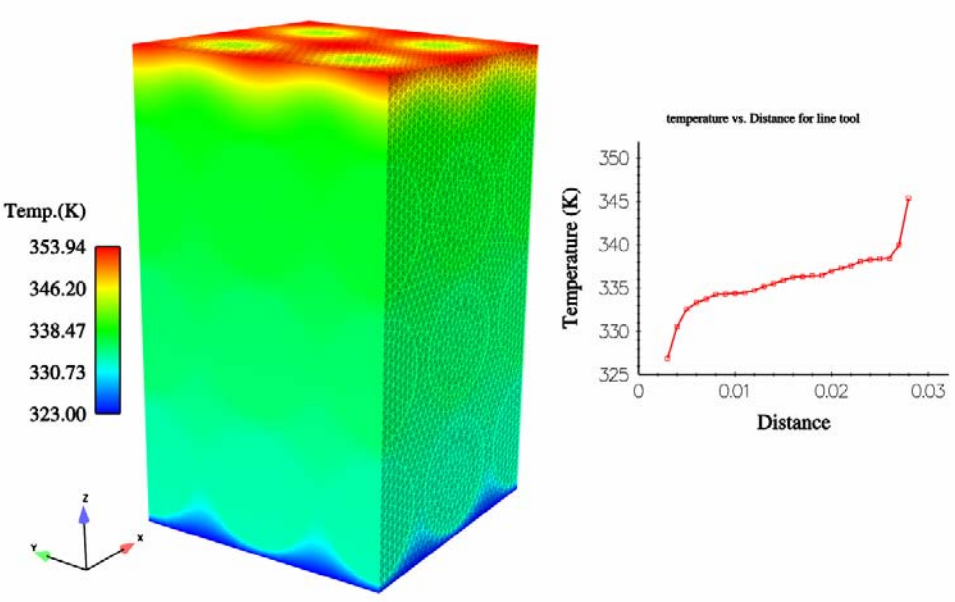

Figure 9. **(Left) Temperature contour plot of the composite with filler distributed in the attached phase; (Right) Axial temperature distribution across the composite.**

2.4.1 Long Chain and High Volume Content

Next the SNL team examined how the effective thermal conductivity of a composite with filler is affected by an increase in the volume content of filler and the creation of more attached particles in a chain. The results of thermal analysis using the Calore finite element code reveals that increasing the volume content of filler will definitely enhance the thermal conductivity of a composite. However, the magnitude of this enhancement is highly dependent on how many filler particles are attached to each other (Figure 10). It would be highly valuable to develop a manufacturing process to create more attached particles and align them in the direction of temperature gradient. Figure 11 plots the calculated thermal conductivity as a function of the number of attached filler particles within a chain. Each curve represents a different volume content of filler in the composite. Creating a longer chain with more particles is an effective way to improve the effective thermal conductivity of the composite. However, it is more effective if the volume content is high or moderately high. For example, at the volume content of 30%, the curve reaches an asymptotic value. On the other hand, at the volume content of 45% or above, the behavior of the top three curves is similar. That is, a longer chain with more attached particles aligned in the direction of temperature gradient is more effective for heat conduction.

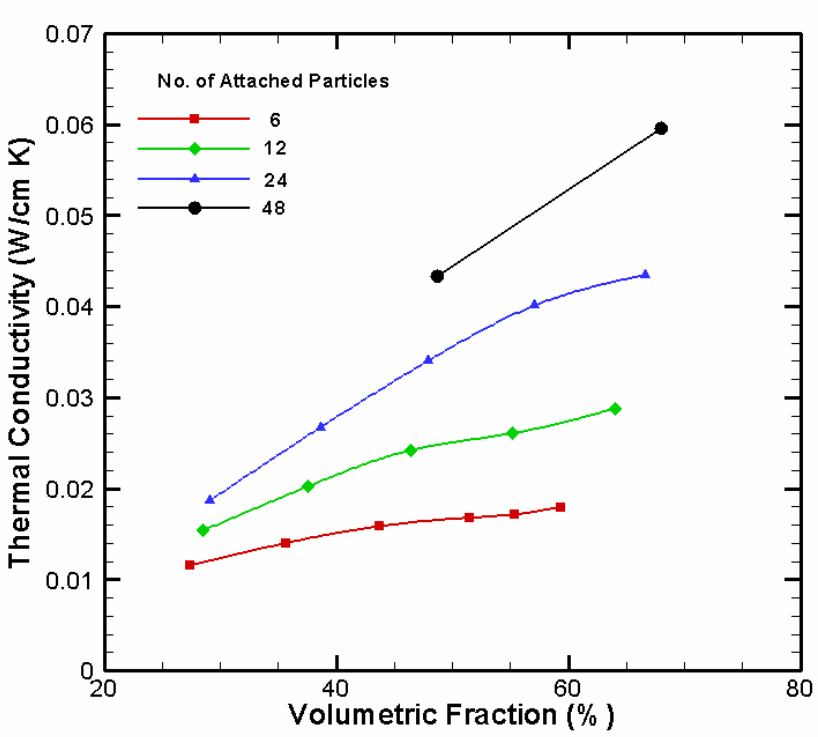

Figure 10. Plot of the calculated thermal conductivity as a function of volume fraction of filler in the composite for filler chains with a different number of attached particles.

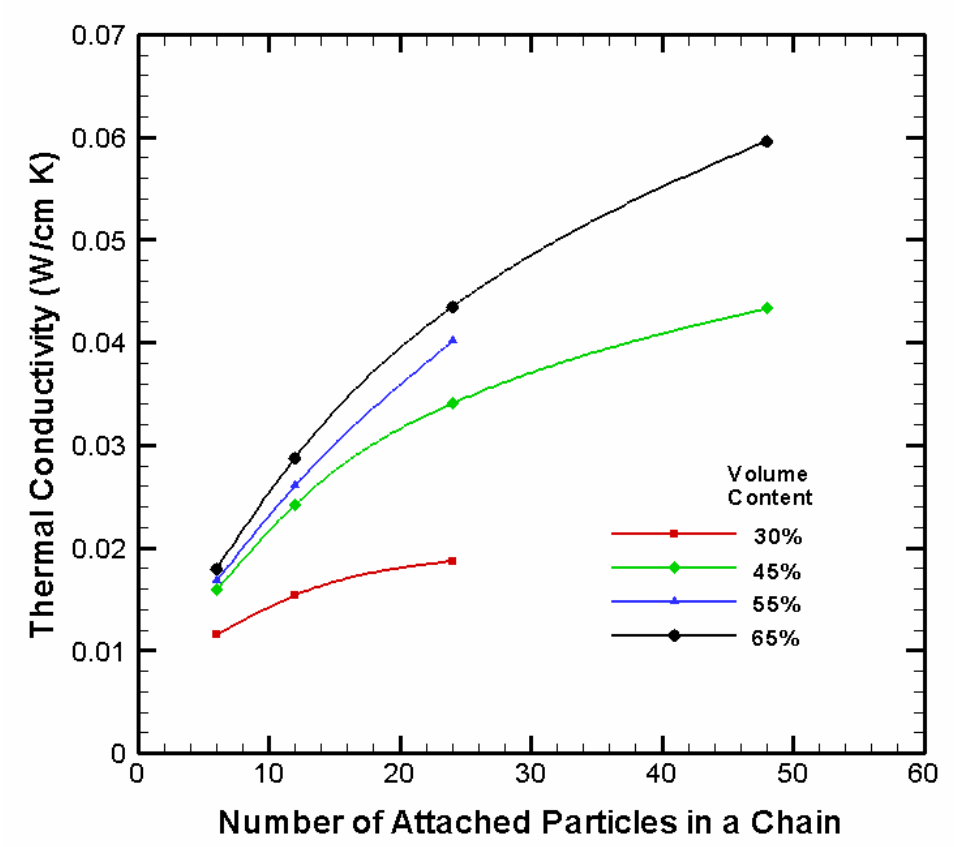

Figure 11. Plot of the calculated thermal conductivity as a function of the number of attached filler particles within a chain for different volume content of filler.

This thermal analysis indicates that when designing a TIM with a better heat conductivity, it is important to incorporate a high content of filler and create chains of attached particles aligned in the direction of temperature gradient. In practice, it is difficult to achieve this goal because of the limitation in manufacturing capability. Moreover, designing a composite with high volume content of filler and long chain of attached particles may work well for heat conduction, but it may not lead to a higher mechanical strength of material. Additional mechanical analysis of the composite with this structure is definitely needed.

2.4.2 Comparing with Agari Experiments

This section assesses the computational model and the Calore code capability by comparing predictions against experimental data. Two Agari test results are used for this assessment. The first set of data is from Agari (1985), in which polyethylene is the adhesive polymer and graphite particles of 44 μm in diameter as the filler. The volume content of filler in the test is relatively low. Calculated results from different models are plotted against experimental data shown in Figure 12. The first two curves are the computational predictions in which the filler is either in the dispersed or attached phase. The present result for the dispersed phase compares reasonably well against the Maxwell-Eucken correlation and also the experimental data at the volume content of 10% or smaller. For the attached phase, the computational model is set up with chains

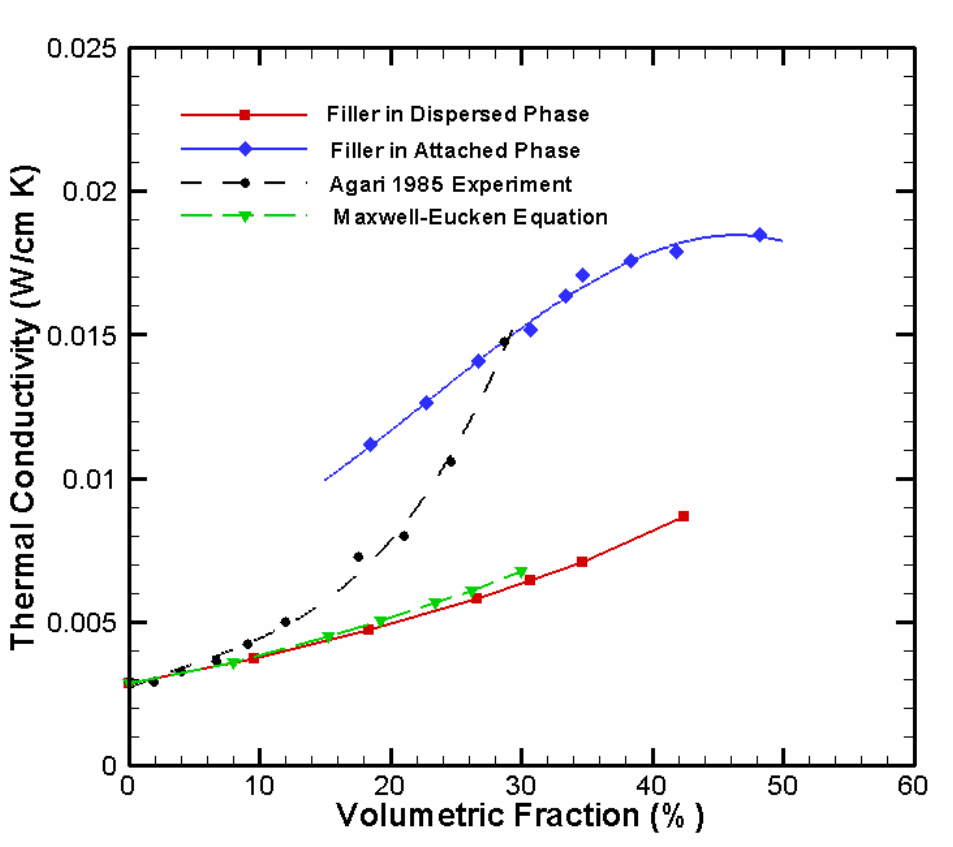

Figure 12. Comparison of the calculated and measured thermal conductivity of composite materials with different filler volume contents as in Agari (1985).

of six attached particles aligned in the direction of temperature gradient. The alignment of attached particles is similar to the lattice structure, as shown in Figure 7. The calculated thermal conductivity from both computational models can be used to interpret the experimental data. This implies that the composite material in the test with the filler volume content between 10% and 30% has particles in the attached phase and the average number of attached particles in a chain is likely less than six.

Agari (1990) measured the thermal conductivity of several composite materials with the volume content of filler as high as 65%. The test result in which the adhesive polymer is polyethylene and the filler is alumina of 65 μm in diameter is used to evaluate the computational models and assess the code performance. At high volume content, many filler particles in these composites are likely attached with others. However, it is relatively difficult to determine the structure and orientation of these attached particles. For example, is there a formation of chains of attached particles? If yes, what is the average number of attached particles in a chain? In the previous section, the effective thermal conductivity of a composite made of similar materials (i.e. polyethylene and alumina) was calculated for different volume contents of filler and for different variations of chains of particles (Figure 10 and 11). In order to compare these predictions against experimental data, it is assumed that for a specific volume content of filler, there exist a characteristic average number of attached particles in a chain. This number will increase with a higher volume content of filler. Table 2 lists the values of these two parameters: filler volume

content and average number of attached particles used to calculate the effective thermal conductivity for model assessment. Figure 13 plots the code predictions versus measurement, showing a reasonably good agreement between calculations and data.

Table 2. The Average Number of Attached Particles per Chain for Different Filler Volume Contents Used to Generate the Computational Model for Code Assessment.

Volume Content	26.32%	43.69%	55.13%	66.60%
Average Number of Attached Particles per Chain	4	6	12	24
Calculated Thermal Conductivity (W/cm K)	0.002244	0.003788	0.006225	0.010388

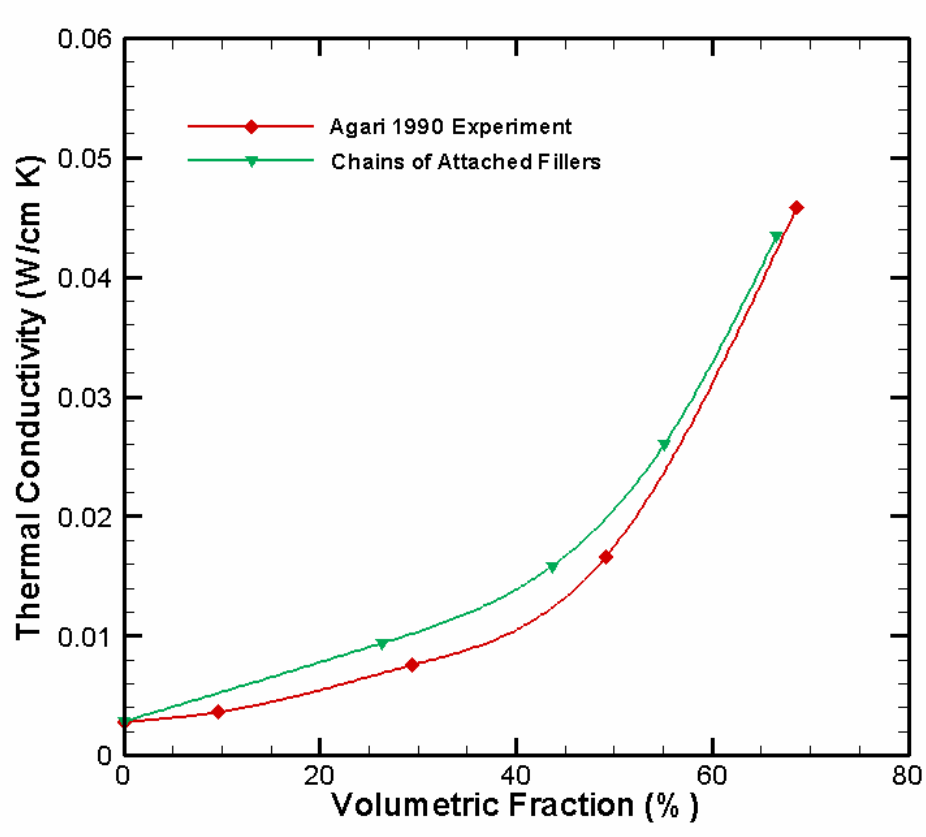

Figure 13. Comparison of the calculated and measured thermal conductivity of composite materials with different filler volume contents as in Agari (1990).

2.4.3 Effect of Contact Resistance

For the modeling results presented so far, the contact resistance between adhesive polymer and filler particle is assumed to be zero. The effect of nonzero contact resistance between two dissimilar materials has been analyzed; our interest is to evaluate the contact resistance between adhesive polymer and filler on the overall effective thermal conductivity of the composite.

The cases analyzed have the following conditions: volume content = 40%; contact conductance between adhesive polymer and filler particles, h =40 W/cm^2 K. For those cases in which the filler particles are in contact with each other to form a string of particles, the effective thermal conductivity of the composite does not change drastically if the contact resistance between polymer and filler increases significantly. For example, for a string of 12 contact filler particles, the calculated effective thermal conductivity of the composite decreases by less 4%, from 0.0203 to 0.0195 W/cm K if the contact conductance between polymer and filler decreases to 40 W/cm^2 K. However for those cases in which the filler particles are dispersed evenly without any contact with any other particle, the effective thermal conductivity of the composite does change drastically. Since our interest is to enhance heat transfer across the TIM, we will only focus on those situations in which the filler particles are likely in contact with one another.

3. SYNTHESIS AND PURIFICATION OF SILVER NANOPARTICLES

3.1 Introduction

The primary aim in the synthesis of silver nanoparticles was to reproducibly synthesize silver nanoparticles in batches of about 1 gram. While a gram of material does not sound like much, for nanoparticle syntheses, this is a very large batch. Nanoparticles are typically produced in dilute solutions with large quantities of surfactants present to trap the material in a non-equilibrium nanoparticle structure. The focus, then, was on finding a highly scalable and repeatable method for this nanoparticle synthesis.

Syntheses of noble metal nanoparticles are typically based upon the reduction of metal salts with a hydride reducing agent. The salt used most commonly is a chloride, while the reducing agent depends upon the solvent system chosen. There are two choices in solvents systems commonly used: an anhydrous organic solvent or a water based synthesis that may or may not include an organic phase. For the synthesis of large quantities of materials, the use of water has numerous benefits. The dissolution of metal salts in water is fast and easy, and the quantity that can be dissolved is substantial. Phase transfer of the salts to an organic phase followed by the addition of an aqueous reducing agent creates an interfacial reaction that can control the kinetics of the reaction. The limited rate of reaction in the interfacial reaction allows the reaction to be scaled up substantially to produce large quantities without problems associated with removing heat from the exothermic reaction. The interfacial reaction also maintains its reaction kinetics in larger reactions, meaning the reaction can scale up without changing the particle size distribution, which is kinetically controlled in these reactions.

3.2 Experimental

A modification of the Brust procedure (Brust 1995) was used to prepare the gold nanoparticles. The procedure consists of a two phase system, where an aqueous gold salt is transferred to a toluene phase by a phase transfer reagent (tetraoctylammonium bromide). The gold is then reduced, in the presence of alkanethiols, by an excess of aqueous sodium borohydride. The gold is fully reduced to metallic gold, and the surfaces of the gold agglomerates are promptly passivated by the alkanethiols present in solution. The alkanethiols self-assemble to form a monolayer on the gold surfaces, producing a stable dispersion of nanoparticles in the toluene phase. The particles can be precipitated, redispersed in organic solvents, and stored as a solid for months without change in chemical composition or structure. The nanoparticles formed by this method have been well characterized, and can be prepared in a range of sizes by varying the gold-to-surfactant ratio. In this synthesis, a gold:surfactant ratio of 1:1 was used, which has been shown in the literature to produce particles with a radius of approximately 1 nm.

This procedure was modified to produce silver nanoparticles, and new methods of purification were developed to ensure the absence of ionic species. In a typical synthesis, 2 g of silver nitrate are dissolved in 50 mL of water and a solution of 6.5 g of tetraoctylammonium bromide in 150 mL of toluene is added. The two phases are vigorously stirred together, and the silver ions are transferred to the organic phase. Dodecanethiol (156 mg) is added to the mixture, and then a solution of 4 g of sodium borohydride in 250 mL of water is added over the course of approximately 30 seconds to reduce the silver, forming the nanoparticles. This procedure has

been shown to make approximately 5 nm silver particles (Figure 14). These nanoparticles contain about 50% silver by mass, with the balance of the mass due to bound surfactant.

3.3 Results and Discussion

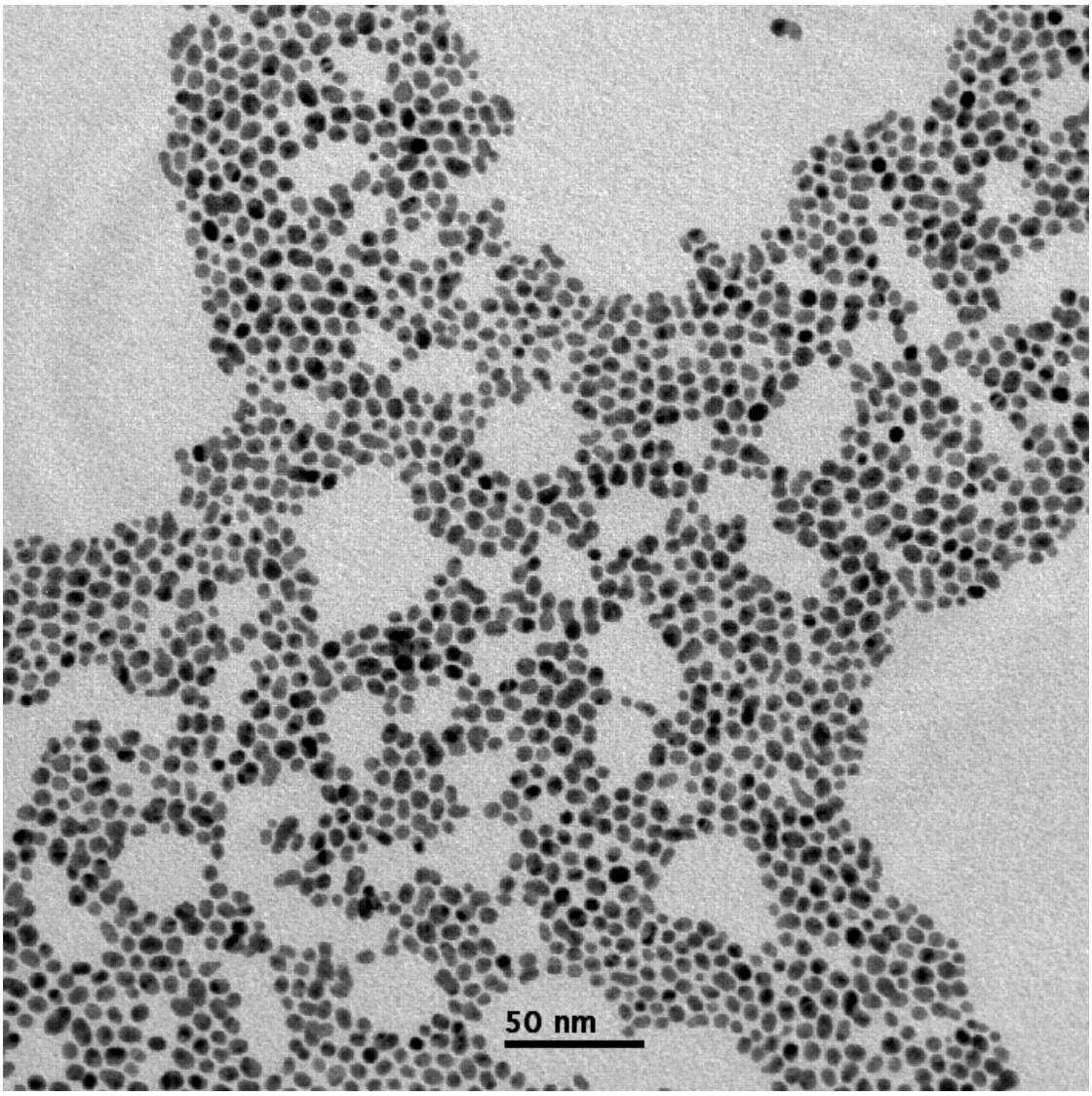

Figure 14. Transmission electron micrograph of approximately 5 nm silver nanoparticles. The particles have a narrow polydipsersity for particles produced in such a large quantity.

The requirements for testing metal nanoparticles as TIMs are quite stringent. They must be reasonably uniform in size, very well passivated, and able to be produced in relatively large quantities (hundreds of milligrams at a minimum). A number of syntheses are known to produce thiol-passivated nanoparticles that meet the first three requirements, but production of large quantities of materials is difficult and drove the selection of synthetic techniques.

A two-phase synthesis, utilizing a cationic phase transfer reagent, was chosen for the preparation of nanoparticles due to its ability to produce large quantities of nanoparticles of sufficiently high quality. The reaction is highly scalable and a single reaction with about 600mL of total volume can produce around a gram of purified nanoparticles. Another advantage of the two-phase synthesis method chosen is that the vast majority of ionic byproducts from the reaction are extracted to the aqueous phase during the course of the reaction. This simplifies further purification and removal of conducting impurities, which is critical for accurate thermal measurements. Size control in this synthesis is achieved by changing the amount of silver salt and reducing agent while holding all other reagents constant, where increasing quantities of silver salt yield larger particles.

Since purity is of paramount importance, a number of schemes were employed to clean the samples of impurities. After synthesis and the initial precipitation of the particles, compressed films were shown to have very low electrical resistivity. Freezing the sample in liquid nitrogen greatly suppressed the conduction, implying that it was ionic conduction due to salt impurities. A lengthy solvent washing procedure was devised to remove ionic impurities. The precipitated nanoparticles, collected on a filter, were washed four times, alternating between water and methanol. To ensure removal of conducting impurities, it was necessary to redissolve the particles in toluene, precipitate, and wash them again. This procedure served to remove both excess surfactant and ionic reaction byproducts, demonstrated by a lack of ionic conduction. Thermogravimetric analysis also verified the absence of these species (Figure 15).

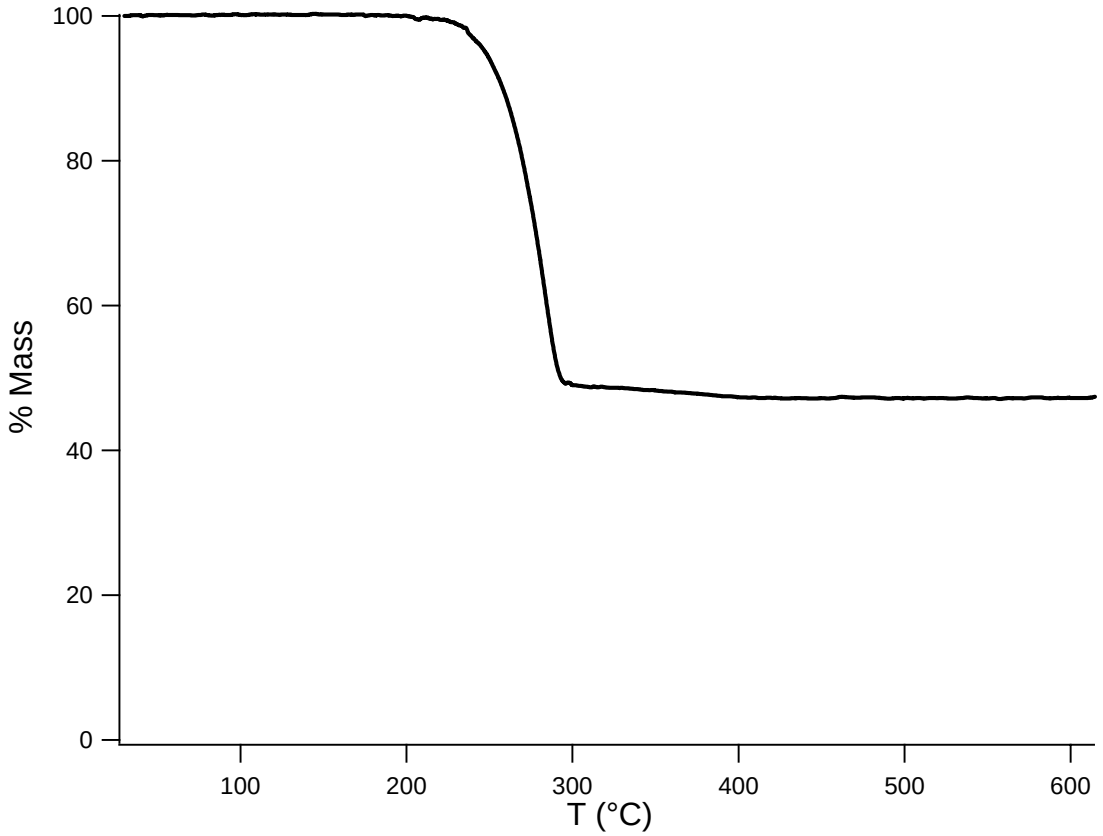

Figure 15. Thermogravimetric analysis of purified silver nanoparticles under nitrogen.

The single weight-loss event attests to the purity of the particles, indicating that there is only one volatile species present. The loss of mass occurring at the temperature dodecathiol would be expected to boil off.

The purity of these samples is so critical that attempts were made to remove all extraneous materials. The precipitation and solvent washing procedure described previously were shown to be sufficient at removing ionic impurities, but trapped solvent molecules could also strongly impact final properties, as well as overestimate the silver loading. An extremely effective method of removing trapped solvent is freeze-drying. SNL's freeze-drying procedure involved dissolution of the sample in a minimum of benzene, then doubling that volume to ensure good solubilization. The sample was then frozen in a round bottom flask, connected to a Schlenk line, and the flask evacuated. Vacuum was applied until the sample held a vacuum of below 10^{-2} torr. Freeze-drying of the particles produced an extremely fine black powder that could easily be handled and weighed. Very serious conduction problems were encountered in these freeze-dried samples, as well as difficulty redissolving them. Thermogravimentric analysis confirmed that these particles were affected by the freeze-drying procedure. Not only was residual solvent removed, but also a substantial portion of the alkanethiol capping layer. The removal of a portion of the dodecanethiol during the freeze-drying process was a surprise, but can easily be rationalized. Freeze-drying is an effective method for removing solvent because since the solution remains frozen during the course of the drying the removal of solvent by sublimation produces an extremely porous material. The high surface area allows for faster sublimation of volatile species. The dodecanethiol is apparently sufficiently volatile, even when bound to a gold substrate, that a substantial portion is removed during freeze-drying. This is likely exacerbated by the fact that freeze-drying proceeds progressively from the outside of the sample, so that some nanoparticles near the outer edge of the frozen plug spend a number of hours under vacuum without a protective layer of solvent. The exact portion of thiol removed during freeze-drying was highly variable, seeming to depend upon the exact freeze-drying conditions, as well as the location within the sample from which an aliquot was taken. What was consistent, however, was the removal of a portion of the thiol made the particles very difficult to redissolve. For this reason, freeze-drying of the particles to remove residual solvent was abandoned.

Residual solvent remained a concern, but a more innocuous method of removal was desirable. Residual solvent was removed by placing the sample under vacuum for approximately one hour. This proved sufficient to remove the vast majority of the highly volatile solvents used, without removing any alkanethiol or damaging the particles in any other way.

4. SUMMARY

The focus of the nanoparticle synthesis was to create the nanoinclusion candidate process for the incorporation into a TIM planned for the second year. Efforts were made to control size distribution for particle materials that SNL predicts will be compatible with the metallic particles used to load the current polymer epoxies. Since silver is easy to work with for nanoinclusion and possesses a sufficiently large thermal conductivity, it was used as the baseline material for synthesis. The results of nanoinclusions will be reported in Part 2 of this report.

A set of computational tools developed at SNL were applied to model the heat conduction across the TIMs and calculate the effective thermal conductivity of the composite for different volume contents of filler. The thermal analysis indicates that when designing a TIM with a better heat conductivity, it is important to incorporate a high content of filler and to create chains of attached particles aligned in the direction of temperature gradient. In practice, it is difficult to achieve this goal because of the limitation in manufacturing capability. Moreover, designing a composite with high volume content of filler and long chain of attached particles may work well for heat conduction, but it may not lead to a higher mechanical strength of material. Additional mechanical analysis of the composite with this structure is needed.

5. REFERENCES

1. Ravi Mahajan, Raj Nair, Vijay Wakharkar, Johanna Swan, John Tang, and Gilroy Vandentop, Intel Technology Journal **6** (2), 62 (2002).

2. Ravi Prasher, International Journal of Heat and Mass Transfer **48,** 4942 (2005).

3. Y. Agari and T. Uno, J. Appl. Polym. Sci. **30**, 2225 (1985).

4. Y. Agari, A. Ueda, M. Tanaka, and S. Nagai, J. Appl. Polym. Sci. **40**, 929 (1985).

5. Y. Agari, M. Tanaka, S. Nagai, and T. Uno, J. Appl. Polym. Sci. **32**, 5705 (1986).

6. Hiroshi Hatta and Minoru Taya, J. Appl. Phys. **59**, 1851 (1986).

7. L. C. Davis and B. E. Artz, J. Appl. Phys. **77**, 4954 (1995).

8. D.P.H. Hasselman and Lloyd F. Johnson, J. of Composite Materials, **21**, 508 (1987).

9. J.F. Shepherd, "CUBIT Mesh Generation Toolkit," SAND2000-2647, Sandia National Laboratories, Albuquerque, New Mexico 2000.

10. S. W. Bova, K. D. Copps, and C. K. Newman, *Calore: A Computational Heat Transfer Program, Volume 1, Theory Manual,* SAND2005-0551, Sandia National Laboratories, Albuquerque, New Mexico, 2005.

11. Carter Edwards and James R. Stewart, "SIERRA: A Software Environment for developing Complex Multi-Physics Applications," in K.J. Bathe, editor, *First MIT Conference on Computational Fluid and Solid Mechanics*, Elsevier Science 2001.

12. M. Brust, J. Fink, D. Bethell, D. J. Schiffrin, and C. Kiely, J. Chem. Soc. – Chem. Comm., **16**, 1655 (1995).

APPENDIX A – SETUP FOR CALCULATING HEAT FLUX

The Sandia thermal analysis code (CALORE) has been applied to calculate temperature distribution across a common thermal interface material (TIM). This TIM (silicone as the adhesive amorphous matrix material, mixing in with silver particles of 10 microns in diameter) will be considered as the baseline case. The thickness of this interface material has a range between 100 and 800 microns, depending on the number of rows of filler particles. Heat flux is applied uniformly at the top surface such that q"=20 W/cm^2 and the bottom surface is kept at 323 K. Using this boundary condition, the temperature profile at the hot surface can be calculated. In order to determine the effective thermal conductivity of the TIM, the maximum temperature at the hot surface is used. Hence the calculated thermal conductivity may be slightly smaller than the measured value, depending on how the temperature at the hot surface is defined in the experiment. In summary, the comparison between the predictions and measurement is reasonably good.

Distribution

1	MS0123	Donna Chavez, LDRD Office	1011
1	MS0406	Gayle Thayer	5711
1	MS0792	Blake Jakaboski	17152
3	MS0792	Michael Rightley	17152
1	MS0826	Edward Piekos	1513
1	MS0826	Daniel Rader	1513
1	MS0888	Douglas Adolf	1821
1	MS0958	Michael Kelly	2453
1	MS0961	Mark Smith	2450
1	MS0965	Kathryn Hanselmann	9114
1	MS0980	Stephen Gentry	5703
1	MS0980	Toby Townsend	5703
1	MS1070	C. Channy Wong	1526
1	MS1071	Clinton Boye	1720
1	MS1076	Thomas Fischer	1715
1	MS1085	Subhash Shinde	17152
3	MS1245	John Emerson	2453
1	MS1245	David Rae	2453
1	MS1304	Dale Huber	1132
1	MS1349	Frank van Swol	1112
1	MS1415	Robert Hwang	1110
2	MS9018	Central Technical Files	8944
2	MS0899	Technical Library	4536

1 Eric J. Cotts
Physics Department and Materials Science Program
Binghamton University
P. O. Box 6016
Binghamton, NY 13902-6000